Top Curr Chem (2003) 226: 91 – 118
DOI 10.1007/b 10826

Nanocasting and Nanocoating

Rachel A. Caruso

School of Chemistry, The University of Melbourne, Victoria 3010, Australia
E-mail: rcaruso@unimelb.edu.au

The use of organic templates for the controlled structuring of inorganic materials is being widely explored. Two processes, nanocasting and nanocoating, will be discussed in this chapter for the formation of porous metal oxide structures with an emphasis on silica and titania. The difference between the two techniques is that casting is a filling of the porous structure of the organic material whereas coating results in a layer of the inorganic substance on the polymer structure. Following formation of the hybrid, the organic template can be removed, yielding a structured inorganic material. Either an *inverse* replica of the initial structure is obtained after *nanocasting* or a *hollow* replica of the organic results with the *nanocoating* procedure. The initial organic molds considered here are "rigid", preformed matrices or discrete entities that do not require the presence of the inorganic material for producing or maintaining their structure. These range from monolithic materials, including porous polymer gels and colloidal crystals, to organic fibers, crystals, and latex particles. The fabrication methods discussed that are used to obtain the metal oxide structures include sol-gel procedures and the use of preformed metal oxide nanoparticles.

Keywords. Template, Metal oxide, Silica, Porous structures, Sol-gel, Nanoparticles

1 Introduction 92

2 Monolithic Materials and Films 95

2.1 Disordered Structures 95
2.1.1 Polymer Gels 95
2.1.2 Organic Membranes 97
2.2 Ordered Structures 99
2.2.1 Colloidal Crystals 100
2.2.2 Polycarbonate Membranes 104
2.2.3 Biological Assembly 105

3 Hollow Fibers and Threads 105

3.1 Synthesized Fibers 106
3.1.1 Polymeric Fibers 106
3.2 Assemblies 107
3.2.1 Biological Threads 107
3.2.2 Organogelators 107

4 Discrete Entities 110
4.1 Spherical Particles 110
4.1.1 Solid Latex Particles 110
4.1.2 Porous Spheres 111
4.2 Elongated Materials 112
4.2.1 Tubes and Nanotubes 112
4.2.2 Organic Crystals 116

5 Summary 116

References 117

List of Abbreviations

PDMS	Poly(dimethylsiloxane)
PMMA	Poly(methylmethacrylate)
PS	Polystyrene
PVP	Poly(vinyl pyrrolidone)
SEM	Scanning electron microscope
TBOT	Titanium (IV) tetrabutoxide
TEM	Transmission electron microscope
TEOS	Tetraethylorthosilicate
TIP	Titanium (IV) isopropoxide
TMOS	Tetramethylorthosilicate

1 Introduction

Morphological control of materials is required to obtain unique, often advantageous, and enhanced material properties. This chapter reviews recent research on the use of organic templates for the "transcriptive synthesis" [1] of inorganic materials, in particular silica and metal oxides, with controlled structures.

Templating generally requires three steps. First, the choice or preparation of the template, then the formation of a composite consisting of the template and final material, and third the removal of the template, giving the final structured material. Materials formed at step 2 often already have interesting and useful properties making the removal of the template unnecessary:

Step 1	→	Step 2	→	Step 3
Template		Composite		Structured material

Discussing each of these steps in turn, we start with the template. The template itself is a structured object within which, or around which, the second material is formed. The templates discussed in this chapter are organic and of fixed form,

that is, the morphology of the template is apparent without the addition of the inorganic coating or casting substance and there is little change in its structure, except possibly for some expansion and shrinkage, during the templating process.

Templates require certain properties:

1 They have to have a structure that is of interest for the final material.
2 They need to be able to maintain their structure during the templating procedure.
3 If the final material is to be without the template, they need to be easily removed without disrupting the structure.

Polymeric materials are ideal for this application. Numerous morphological variants can be obtained which are of interest, different polymers can withstand a wide variation of conditions, including extreme pH and harsh solvents, and the polymer can be removed by decomposition using solvent, plasma treatment or heating procedures.

The organic templates that will be examined have been categorized according to the final inorganic structure. First, monolithic materials and films composed of both disordered and ordered three-dimensional porous structures are discussed. The formation of these materials requires templates such as polymer gels and membranes that have a bicontinuous pore morphology, and colloidal crystals and membranes, with fixed pore domains (in both size and structure). Then the fabrication of inorganic threads and hollow fibers is considered where polymeric fibers, biological threads, and organogelators act as scaffolds on or in which the inorganic material forms. This is followed by a section on templates composed of discrete entities, which result in hollow spheres and tubular materials. The organic templates in this section are spherical polymers (latex particles) or elongated organic materials such as nanotubes and crystals.

These templates can also be combined with other porogens (such as self-assembled polymers) or techniques to obtain hierarchical pore systems or structured materials on a number of length scales. Examples demonstrating the extension of simple templating to more complex structural control will also be given.

Composite materials can be formed by numerous methods. Two modes in which incorporation of the inorganic material in the template can be achieved will be discussed: sol-gel processes or nanoparticle infiltration. They are both solution methods that can be processed at low temperatures, hence allowing the use of polymeric templates. In the first method the sol-gel chemistry is performed after the incorporation of a metal oxide precursor in the polymer matrix or around the template entities. The second method makes use of preformed metal oxide nanoparticles, which are infiltrated into the organic scaffold or suspended in solution with the individual structures for controlled adhesion.

The sol-gel process involves hydrolysis and condensation reactions of the precursor, where in general (especially for the non-silica precursors) both reactions occur simultaneously [2], forming a metal oxide "polymer" and low molecular weight species (water and alcohol). The shrinkage observed during the sol-

gel process is due in part to the removal of these species [3]. The overall reaction can be summarized as follows:

$$M(OR)_4 + 4H_2O \rightarrow M(OH)_4 + 4ROH$$
$$M(OH)_4 \rightarrow MO_2 + 2H_2O$$

where M represents a group 4 metal and R the alkyl group.

The use of nanoparticles requires the initial synthesis of the nanoparticles, which generally adhere to the template via electrostatic and hydrogen bonding interactions, or on processing of the nanoparticles and template the nanoparticles are physically confined within the template.

For templating in general, the final material can be achieved in a number of ways, including casting, coating, curing, and directed "assembly". This chapter will concentrate on the first two techniques applied on a submicron scale, that is either the template itself or the coating applied to the template is of nanometer proportions. Casting involves the complete filling of the porous system around the template material compared to coating, which results in a thin layer formed on the mold; see Scheme 1.

These processes are conducted with the purpose of generating materials with properties that are dependent on either a combination of the mold and the templated materials, or the structural properties obtained during the templating procedure. For the two techniques focused on in this chapter, nanocasting and nanocoating, the materials obtained on removal of the template resemble the initial template either as structural negatives (casting – gives pores where there

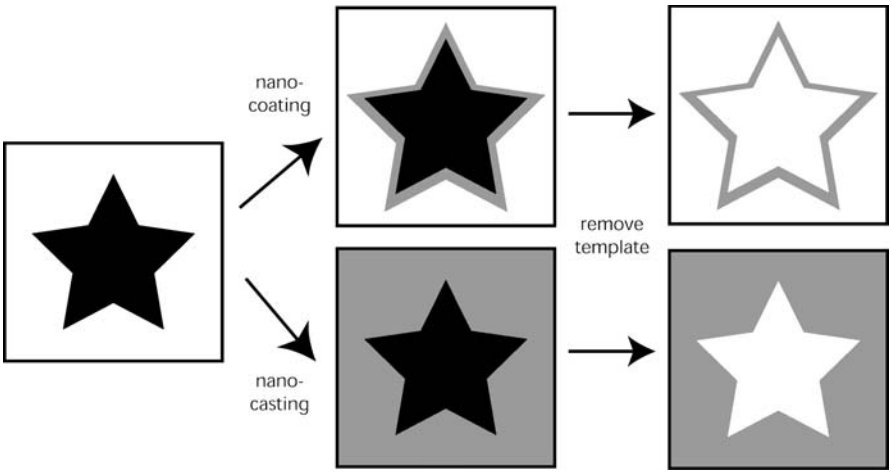

Scheme 1. Templating steps including both casting and coating approaches. Schematic illustration demonstrating the casting and coating of a star-shaped template. The casting technique gives a composite in which the second material fills the area around the mold so that on removal of the mold a structured material is obtained, which is an inverse replica of the initial template. In contrast, coating of the template results in a layer of the second material around the mold, resulting in a hollow replica on removal of the template

was originally template, and solid where there were originally pores) or as hollow structures with similar shape to the initial mold (coating – pores from the original mold are retained, plus additional pores are obtained on removal of the mold). This is depicted in Scheme 1.

The formation of such structured materials for various applications including separation, catalysis, and photonics has led to various activities in the fields of chemistry, engineering, materials science, and physics conducting detailed research on the controlled fabrication and the final properties of such materials. The use of templating procedures, including nanocoating and nanocasting techniques, allows the formation of porous structures with high-level control of the morphology (pore size and structure, as well as over all material shape and size) by a rather simple and efficient process.

Porous materials have been classified by the IUPAC (International Union of Pure and Applied Chemists) to be microporous if the pore size is below 2 nm, mesoporous if the pores have a diameter between 2 and 50 nm, and macroporous if the pore diameters are above 50 nm [4]. This chapter focuses on porous materials with pores in the meso and macro-regime.

2
Monolithic Materials and Films

Large hybrid inorganic/organic materials or inorganic structures can be formed by the use of monolithic templates or stacking of discrete entities into a monolithic structure. The monolithic structures can be disordered systems, such as polymer gels and membranes, consisting of random porous structures that are continuous and therefore can be penetrated by the inorganic material, or they can have ordered, regular pore structures such as the cylindrical pores found in polycarbonate filter membranes or the void spaces remaining on stacking of monodisperse polymer spheres. Ordered structures can also be formed with biological cells and used successfully as templates. The order or disorder of the porous structure and the overall porosity is of importance for their application. The final material retains the outer structure of the mold giving inorganic blocks or films.

2.1
Disordered Structures

The template materials discussed in this section are polymer gels and membranes. These organic matrices show that bulk hybrid or porous inorganic materials can be obtained using sol-gel or nanoparticle infiltration methods.

2.1.1
Polymer Gels

Polymer gels are an excellent example of an organic system that can be morphologically tailored. The synthesis of numerous polymer gels with a wide variation in the pore size and structure, and overall porosity has been achieved

[5, 6]. The choice of surfactant, monomer, and cross-linker gives a range of gels that are stable over significant pH values and that are easily handled with tweezers during the templating procedure. The sponge-like, bicontinuous pore structure makes impregnation procedures possible.

Hybrid metal oxide/polymer monoliths are formed when sol-gel reactions are performed within the pore system of the organic gel [7, 8]. The alcohol soaked polymer gel is simply placed in the liquid precursor and then into an alcohol/H_2O solution for hydrolysis and condensation, which gives an amorphous metal oxide layer on the polymer surface. Heating the hybrid at 450 °C results in removal of the organic template and crystallization of the inorganic material.

"Coral-like" TiO_2 structures have been formed which clearly demonstrate coating of the initial template, an acrylamide/glycidylmethacrylate polymer gel [7]. Highly porous inorganic networks with pore sizes from 100 nm to microns were obtained. The walls, with a thickness of 100–150 nm, are composed of TiO_2 nanoparticles, as can be seen in a thin slice of the sample viewed by TEM in Fig. 1. Variation of the initial polymer gel gives various pore sizes and different surface areas in the final titania structures, as shown in Table 1 [8]. The morphology of the final inorganic material and its properties are strongly dependent on the structure of the initial template. The crystallinity of the nanoparticles in the network (anatase or rutile phase) was determined by controlling the temperature of calcination.

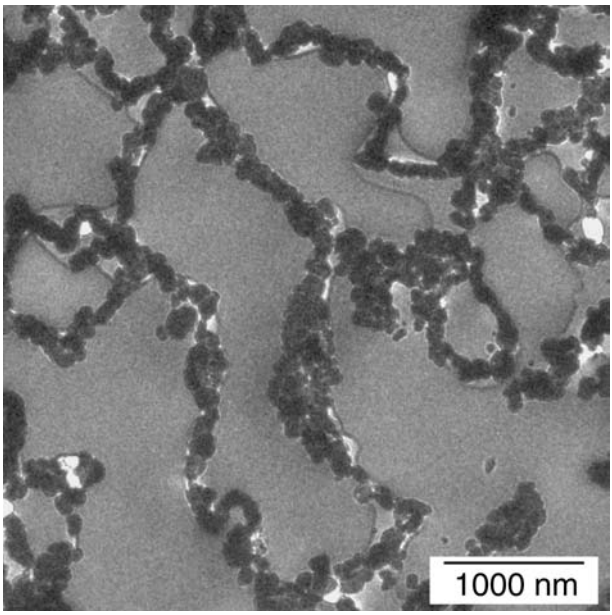

Fig. 1. TEM image of an ultramicrotome of the titania network constructed using a polymer gel template, showing the individual titania nanoparticles of which the structure is composed. Reprinted with permission from [7]. Copyright 2001 American Chemical Society

Table 1. Properties of the titania networks obtained by using polymer gel templates: calculated porosity, surface area obtained from nitrogen adsorption, pore, and titania nanoparticle diameters. Adapted with permission from [8]. Copyright 2001 American Chemical Society

Polymer gel template	Calculated porosity (vol.%)	Specific surface area[a] ($m^2\ g^{-1}$)	Pore diameter range[b,c] (nm)	TiO_2 colloid diameter range[b] (nm)
B561	98	20	70–900	25–175
B562	97	11	100–3000	15–165
T601	99	39	10–325	5–40
B581	98	4.9	200–3000	25–175
B582	98	9.3	25–2300	20–110
CTA1	94	62	5–60	5–30
CTA2	94	76	–	–
SE1	99	49	3–37	10–40
SE2	99	59	5–20	7–20
EK1	–	99	2–100	4–14
EK2	–	54	5–175	7–50
EK3	–	82	3–24	8–45

[a] BET,
[b] TEM,
[c] SEM.

Monolithic zirconia networks can also be formed using a similar procedure giving porous ZrO_2 structures [9]. As the titania and zirconia precursors are miscible, binary inorganic networks of various Ti:Zr ratios could be produced [9]. The crystallinity and photocatalytic properties of the mixed material were studied: X-ray amorphous materials were produced for Ti:Zr ratios of 2:8 to 7:3, and the binary material containing 10% zirconia (the presence of which inhibited crystal transformation to the rutile phase) showed the highest photocatalytic activity for the photodecomposition of salicylic acid and 2-chlorophenol [9].

Similar templates with solvent swelling properties have been used for nanoparticle infiltration [10]. The acrylic acid/2-hydroxyethylmethacrylate copolymer was soaked in a colloidal sol of 4.5 wt%, 8 nm titania anatase particles for 7 weeks. Thermal treatment to remove the organic scaffold and induce condensation of surface hydroxyl groups between contacting nanoparticles, gave porous titania monoliths.

For the production of bulk materials monolithic structures of a desired shape are applied; however, in a number of applications, such as photocatalysis and photovoltaics, film structures are more practical. The next topic discusses the use of membranes with a similar "sponge-like" pore morphology for fabricating inorganic films.

2.1.2 *Organic Membranes*

Membranes such as cellulose acetate or other cellulose derivatives have porous structures that vary depending on the material composing the membrane and

its particle retention diameter. The membranes used as templates have a thickness of ~100 μm. For cellulose acetate membranes (viewing the inner morphology perpendicular to the flow direction (plane) of the membrane) the pore size is relatively homogeneous and the membrane is quite dense. Polyamide membranes, on the other hand, show a distinct gradient in pore size when viewed in the same manner, and have less compact structures. Examining either membrane in the direction of flow shows a substantially different morphology to their respective perpendicular structures. The membranes can be handled with tweezers and due to their overall morphology – very thin compared to the polymer gel blocks – are processed during the templating more rapidly.

Simply soaking the membrane in the liquid precursor and then conducting sol-gel reactions by transferring the precursor soaked membrane into a water/alcohol solution results in an amorphous inorganic coating of the membrane [11]. Alternatively the liquid precursor can be filtered through the membrane, on a Büchner funnel with applied vacuum, followed by the water/alcohol solution giving a similar result. Heating was used to remove the cellulose acetate membranes to give porous metal oxide films of ~80 μm thickness. Such films, made up of crystalline nanoparticles, have been obtained for titania and zirconia. By choosing different particle retention diameters from 450 to 200 nm for the cellulose acetate membranes, the surface area of the resulting titania films was found to increase from 22 to 74 $m^2 g^{-1}$. (The initial surface areas of the 450 and 200 nm diameter particle retention membranes were 5 and 12 $m^2 g^{-1}$, respectively.) This again shows that the morphology of the organic template has an influence on the properties of the final inorganic material.

Polyamide membranes can also be successfully used as templates. Due to the more "open" structure of the polyamide membrane the final inorganic film obtained by nanocoating retains this open structure giving large pores. Nanocasting, however, gives a much denser structure.

Macroporous silica films have been obtained by casting either polyamide or cellulose acetate membranes [12]. Soaking the membranes in a tetramethylorthosilicate (TMOS)/H_2O/HCl solution for 6 min followed by drying between glass plates gave silica filled membranes. The casting is obvious on removal of the membrane. Scanning electron microscopy, SEM, images showed the porous structure in the silica to be of similar morphology to the organic material in the initial membrane; see Fig. 2.

By combining the use of membrane templates with surfactant and polymer self-assemblies as porogens, distinct macro- and mesopore structures can be obtained in the final inorganic films [12]. Mesopores of ~2.7 or 10 nm were produced when using polyoxyethylene(10) lauryl ether (C12E10) or SE30/30 (a block copolymer composed of poly(ethylene oxide) and polystyrene with an average molecular weight of 3000 g mol^{-1} per block) along with the macropores created on removal of the membrane. Again a casting of the membrane is attained. The surface area of the silica film is enhanced by the additional mesopores to surface areas of 849 and 517 $m^2 g^{-1}$ for the C12E10 and SE30/30 porogens, respectively, compared to the surface area of a macroporous silica without mesopores obtained using the same membrane template, 39 $m^2 g^{-1}$.

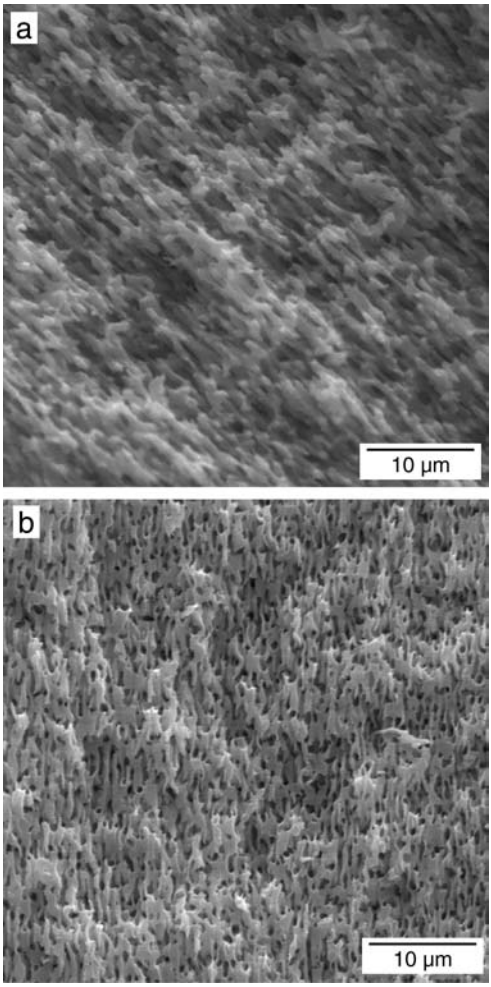

Fig. 2a, b. SEM images of: **a** the membrane template (cellulose acetate); **b** the final silica film. Adapted with permission from [12]. Copyright 2002 Wiley-VCH

2.2 Ordered Structures

Here three template systems are discussed: one that is achieved by assembling monodisperse spheres into a colloidal crystal, the second a membrane (polycarbonate) consisting of cylindrical pores of set dimensions, and the third a biological structure composed of ordered spherical yeast cells. These molds have been cast in most examples, unless blockage of smaller pores prevented the complete filling of larger pores.

2.2.1 *Colloidal Crystals*

Colloidal crystals result from the ordered assembly of particles (see Scheme 2). Polymer spheres with diameters of 100 nm up to microns have been packed using different methods to form films and monolithic structures with quite large, ordered domains. Monodisperse particles give good long range ordering. Casting of these crystals results in inverse colloidal crystals with ordered spherical voids in the inorganic material (Scheme 2). For a review that encompasses the formation of colloidal crystals and their use as templates for the fabrication of a range of porous materials including silica, metal oxides, metals, and polymers see [13], for macroporous metal oxides in particular the reader is referred to [14].

A lot of research has been conducted in the area of ordered macroporous metal oxides obtained from colloidal crystal templates [15–28]. Starting in 1997, Velev et al. [15] showed that such assemblies could be used as templates for the formation of an inverse silica replica. Charged polystyrene (PS) microspheres (200–1000 nm in diameter) were filtered through a smooth membrane forming a film about 10 μm [15] or 20 μm [16] thick composed of closely packed ordered layers of the spheres. The polymeric material was then functionalized with hexadecyltrimethylammonium bromide before a silica solution was filtered through the film. After gelation of the inorganic and drying, the material was calcined to give silica flakes containing uniform pores in an ordered array. The use of different sized latex particles controlled the final pore size (from ~150 nm to 1 μm) with about 20 to 35% shrinkage in the final material.

Using a surfactant-free method [17], PS particles of an average diameter of 470 nm were deposited on filter paper in a Büchner funnel forming a 1 mm thick layer. After soaking the deposit with alcohol the metal oxide precursor (titanium ethoxide, zirconium *n*-propoxide or aluminum tri-*sec*-butoxide) was dripped onto the close-packed assembly of spheres while vacuum was applied. On removal of the organics, the powder particles of titania (anatase phase), zirconia (baddeleyite), or alumina (amorphous) had spherical voids of 320–360 nm in diameter. Shrinkage was 26–32% measured by center-to-center separation between cavities compared with the original latex diameter. The sphere voids were interconnected with "windows" due to the close packing (i.e., points of particle-particle contact) of the organic spheres. Areas of hundreds of microns showed cubic close packing while hexagonal close packing and less regular packing were also obtained. Increased ordering could be obtained with a faster alkoxide flow rate and decreased humidity.

Using a different sedimentation procedure to form the crystals [18] – centrifuging the colloidal suspensions in glass capillaries (0.3 mm thick, 3 mm wide) – polycrystalline sediments larger than 10 mm in length were formed. The template was penetrated with tetrapropoxy-titanate in ethanol under N_2 before being exposed to atmospheric moisture and drying. The procedure was repeated a number of times depending on the titania precursor to ethanol ratio. The PS spheres (with diameters between 360 nm and 3 μm) were removed by heating at 450°C, giving a hexagonal pore pattern in the titania with lattice parameters about 33% less than the original colloidal crystal.

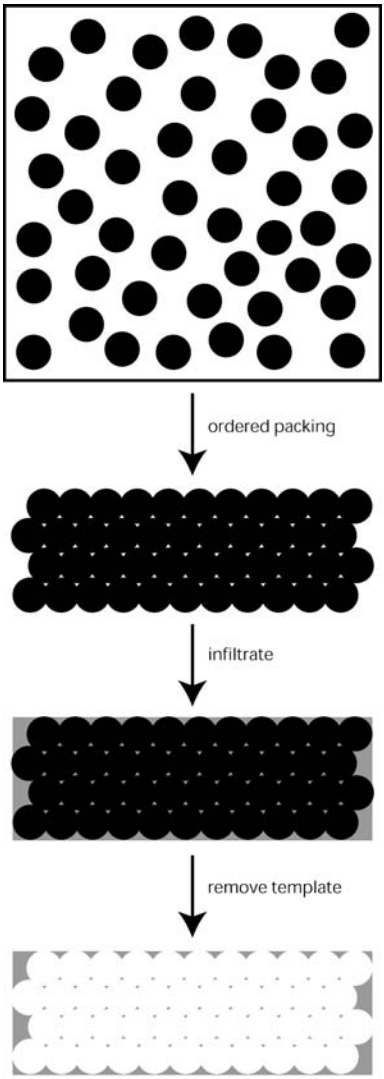

Scheme 2. Formation of colloidal crystals and their use as templates. A colloidal dispersion containing monodisperse particles undergoes controlled filtration, centrifugation, dip coating, sedimentation, or physical confinement, which results in ordered packing of the particles with void spaces between them. By infiltrating these spaces with precursor solution or preformed nanoparticles the hybrid material is formed. Removal of the polymer template (using solvent (toluene) or heating techniques) gives an inverse replica with air-filled, interconnected voids of monodisperse size, which is dependent on the initial particle size

Colloidal crystals have been combined with amphiphilic block copolymers and micromolding (the use of molds that are micron-scaled) to produce patterned silica with hierarchical pore structures [19]. The structure control displayed in this example was on three discrete length scales: 10 nm from the block copolymer (Pluronic F127 or P123), 100 nm due to the latex spheres, and the micromolding gave order in the micron domain. A poly(dimethylsiloxane), PDMS, mold with open ends was placed on a substrate so that a drop of the latex colloidal solution placed at one end could fill the channels, where upon drying the particles organized into a close-packed array. The sol-gel precursor and block co-polymer were mixed and filled the latex voids in the micromold channels by capillary action. After condensation of the silica precursor the PDMS mold was removed and the hybrid calcined at 450°C for 2 h in air to remove the latex and the block copolymer. Isolated patterned structures could also be obtained by placing the mixed sol-gel/block copolymer and latex suspension on a substrate before applying the PDMS mold.

Xia and co-workers have constructed a cell for ordering PS spheres [20]. This consists of two glass substrates framed with photoresist which contains outlets that allow drainage of solvent while retaining the PS spheres which pack to a highly ordered array with applied gas pressure and sonication. Repeated precursor/alcohol solution infiltrations were conducted to achieve filling – as complete as possible – of the voids [29]. Etching of the PS by dissolving in a toluene bath gave 3D porous titania and silica membranes with long-range periodic structure. Although organic inverse replicas with open pores on the membrane surfaces (due to template contact with the substrates) are achieved on removal of the template and substrates [30, 31], the inorganic membranes were too fragile to be taken from the cell support [29].

Holland et al. extended the possible oxide structures to include not only silica, mesoporous silica, titania, zirconia, a yttria stabilized zirconia, and alumina but also oxides of W, Fe, V, and Sb [21]. These latter transition metals formed less ordered structures, containing areas of non-porous material. Different dilutions of alkoxide in alcohol resulted in various inorganic loadings, and moderate control in the wall thickness and window sizes between spherical voids [21]. SEM images of a series of macroporous titania structures obtained with different alkoxide dilutions in ethanol are shown in Fig. 3. Gundiah and Rao have also prepared macroporous materials of ternary mixed oxides, $PdTiO_3$ and $Pb(ZrTi)O_3$ [22].

Further extension of the sol-gel and colloidal crystal templates include control of the outer shape of the colloidal crystal by assembling the PS particles in an aqueous droplet at the air/oil interface [23]. The assemblies then have regular shape (on the length scale of a few millimeters): spheres, ellipsoids, and concave disks. This was controlled by the addition of surfactant and an applied electric field. The cubic close-packed, ordered macroporous titania or silica obtained had similar outer shape as the template.

Preformed metal oxide nanoparticles have also been used in the formation of inverse colloidal crystals [24–26]. Slurries of titania nanocrystals and the PS spheres are dropped onto a glass substrate and dried slowly (over 24 h) [24]. After pressing (cold isostatic press) the film is slowly heated to 520 °C to remove the PS and produce a titania matrix of ≥10 μmx10 mmx2–3 mm with ordered

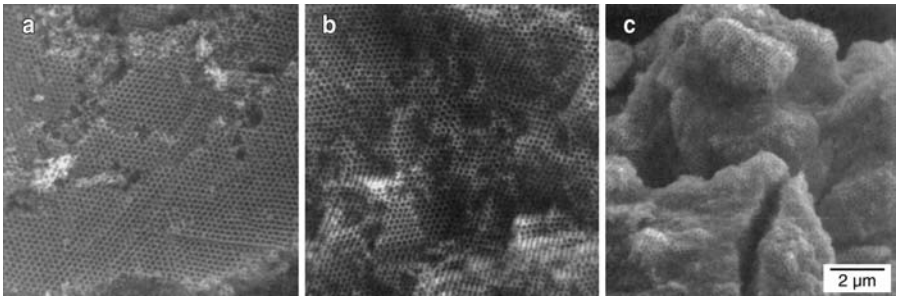

Fig. 3a–c. SEM images of macroporous titania samples synthesized from alkoxides at various dilution levels. The fractions of titanium ethoxide (TET) in ethanol are: **a** 100% TET; **b** 43% TET; **c** 14% TET. The *scale bar* shown corresponds to all of the images. Reprinted in part with permission from [21]. Copyright 1999 American Chemical Society

domains extending from 50 to >100 µm. Windows between sphere voids are also obtained using this method, indicating close packing of the PS, thereby forming an interconnected porous structure in the final inorganic material. Substantially less shrinkage was observed using the preformed nanoparticles with a linear shrinkage of about 6% (compared with 20–35% with the sol-gel approach).

To obtain larger samples Subramania et al. [25] produced samples by slowly drying mixed PS and silica or titania nanoparticles in a glass vial, which results in pieces about 2.5 mm×2 mm×6 mm composed of three regions: a top layer of ordered PS with inorganic particles in the voids, a thin middle layer of ordered PS, and a bottom layer of inorganic nanoparticles. Silica or anatase TiO_2 macroporous structures have been obtained. With further heat treatment (above 850°C) of the titania sample, conversion of anatase crystals to the rutile phase and the resulting crystal growth leads to disruption of the macropores, as is commonly observed.

Highly ordered SiO_2 and TiO_2 macroporous materials can be obtained on a substrate by using a solvent evaporation or "vertical deposition technique" [27, 28]. The PS spheres (406 nm) and SiO_2 (7 nm) or TiO_2 (13 nm) nanoparticles are mixed at a concentration ratio of 1:1 in a vial into which a glass substrate is immersed. Leaving the vial in a constant temperature (50°C) and humidity (30%) chamber leads to the cooperative assembly of the PS and nanoparticles on the substrate with solvent evaporation. Films of 0.5 cm^2 are formed over 24 h. Removal of the PS leaves highly ordered (extending more than 100 µm) porous inorganic materials.

Polymer spheres have also been used for the formation of non-ordered porous systems in inorganic structures and such structures are being tested in applications such as bone tissue implants [32]. Below are examples of casting of discrete entities to form inorganic monoliths or film structures using either sol-gel or nanoparticle infiltration.

Suspensions of polymer spheres of various diameter and surface functionality were templated to produce monolithic silica containing dispersed spherical voids [33]. The pH of the aqueous latex solution was decreased to 2 before the

addition of the silica precursor (TMOS). After removal of the methanol and aging, the latex was pyrolyzed by calcination at 450°C, forming a monolith with spherical pores "possessing a liquid-type interparticular order". Bimodal pore sizes have also been prepared in the silica by the simultaneous templating of latex spheres and a liquid crystalline surfactant phase [33]. Hence, silica materials with spherical pores and a range of pore sizes and density could be obtained. The surfactant assembly controls the size and connectivity of the mesopore system, while the additional spherical pores are obtained by the presence of the polymer particles.

Macroporous titania films have been prepared on titanium surfaces [32] using PS spheres (0.5, 16, and 50 μm in diameter) with TiO_2 particles (39 nm). A slurry of the mixed PS and TiO_2 particles was spread on the titanium substrate and dried slowly (1 day). After heating to 450–950°C, titania with a disordered pore structure was obtained with a thickness of 1 to 0.1 mm on the titanium.

Quite a different approach is to use an inorganic (silica) colloidal crystal to form a polymeric material with ordered spherical voids that can then act as a template for the fabrication of other inorganic materials. Such macroporous polymer materials with ordered spherical voids can be obtained by templating monodisperse silica spheres [34]. For example, a poly(methylmethacrylate), PMMA, mold infiltrated with liquid precursors can be used for the fabrication of monodisperse (5%) inorganic spheres of titania, zirconia, and alumina. The inorganic oxide does not adhere to the PMMA surface but comes away, and therefore complete filling of the voids in the macroporous polymer can be achieved by successive precursor infiltrations. Using PS molds the inorganic material coats and adheres to the template surface, therefore giving hollow spheres of TiO_2, ZrO_2, and Al_2O_3. The wall thickness of the sphere is controlled by the number of coatings. Using this method it is also possible to construct binary metal oxide hollow spheres by successive deposition of different metal oxide precursors, such as Al_2O_3 followed by ZrO_2 [34]. The macroporous polymer template can be deformed by heating the mineral oil filled mold above the glass transition temperature of the polymer, stretching the polymer, and then cooling quickly while in the deformed state. This produces different shaped template voids, such as oblate or ellipsoidal, which can be templated in a similar fashion.

2.2.2 *Polycarbonate Membranes*

Martin and coworkers have demonstrated the use of cylindrical-pored templates for the preparation of tubes and fibers composed of metal oxides, metals and polymers [35, 36]. Track-etching of polycarbonate films gives membranes with cylindrical pores that are randomly distributed across the membrane. The pore diameters are monodisperse and, in the example described here, are 600 nm. Lakshmi et al. have used these membranes for the preparation of vanadium oxide fibers [36]. The pores of the organic filter were filled with vanadium(V) triisopropoxy oxide in an argon atmosphere. Exposure to air at 60°C induces hydrolysis of the precursor before an oxygen plasma is used to remove the polycarbonate. The crystalline alpha phase vanadium oxide (V_2O_5) fibers obtained by this

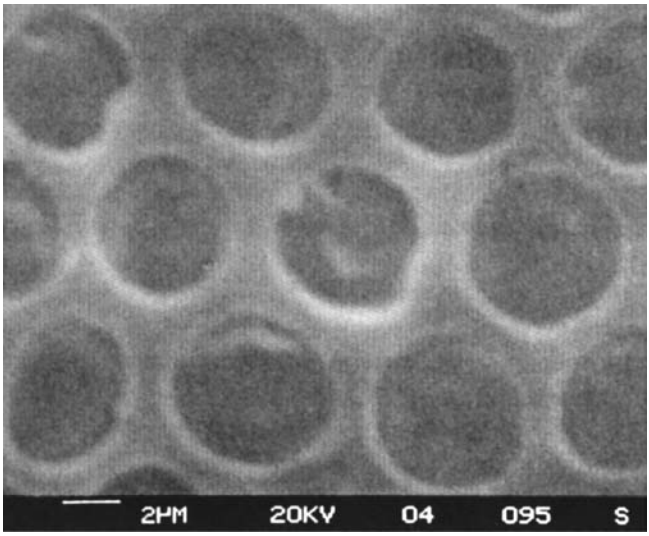

Fig. 4. Scanning electron microscopy image of the silica film templated by spherical cells. Reprinted with permission from [39]. Copyright 2000 American Chemical Society

casting method are monodisperse and protrude from a surface V_2O_5 film. These films have been assessed for reversible lithium ion intercalation [37, 38].

2.2.3
Biological Assembly

Self-organization of cell aggregates can result in ordered templates for replication. An example of spherical yeast cells is given here. The yeast cells can be coated on substrates to give films containing ordered packing of the cells, similar to that obtained in the preparation of colloidal crystals.

As for the preparation of colloidal crystals using polymer spheres, the monodispersity of the cells strongly influences the order of the material. Hence yeast cells were carefully grown to form spherical cells of similar diameter. These cells were dip coated with a silica sol on a microscope slide [39]. A monolayer of the cells arranged in a hexagonal close packing form on the microscope slide. The interstitial sites between the cells contained silica, an SEM image of the film is shown in Fig. 4. The cells remain alive and such films have potential applications in catalysis and as sensors.

3
Hollow Fibers and Threads

Fibrous templates give rise to hollow fiber materials when the nanocoating technique is applied. This is demonstrated below for polymer fibers, a bacterial assembly, and organogelators.

3.1
Synthesized Fibers

Here the use of polymer fiber templates prepared using an electrospinning technique [40, 41] is described. The polymer melt, or a polymer solution in dichloromethane, was expressed through a syringe while a potential was applied between the metal syringe tip and a plate under the collection substrate. The fibers formed using this method can be varied widely in their composition, diameter, and surface morphology. Either nanocoating or nanocasting could be achieved by the sol-gel method, depending on the concentration of the precursor solution.

3.1.1
Polymeric Fibers

Two polymer fibers are discussed: poly(L-lactide) fibers with diameters of 1–3 μm (the majority were about 1–1.5 μm) that had oval indentations on the surface (Fig. 5a), and nylon fibers with diameters of 600 nm and comparatively smooth surfaces. During the electrospinning process the fibers were formed on top of each other in a fibrous mat.

The use of such micron-sized polymeric fibers as templates with the sol-gel templating technique has proved successful in showing the ability to mimic even nanoscale surface morphologies [42]. Applying a dilute titania precursor solution (TIP:isopropanol ratio of 1:19, by volume) and drying in a vacuum desiccator, followed by calcination, afforded TiO_2 tubes of slightly decreased diameter than the original fibers. This indicated successful coating of the tubes. Transmission electron microscopy, TEM, analysis of the inorganic product showed the tubes to have nodules of similar size to the original indentations in the polymeric fiber (Fig. 5b).

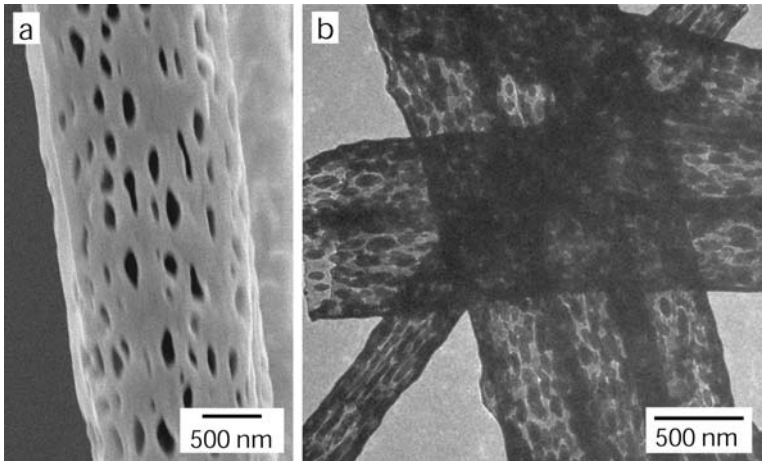

Fig. 5. **a** SEM image of an initial polymer fiber. **b** TEM image of the titania tubes. Adapted with permission from [42]. Copyright 2001 Wiley-VCH

Applying a similar method to the nylon fibers with a more concentrated precursor resulted in films containing a hollow morphology on removal of the fibers. Hence in this case a casting of the fibrous mat was attained. It was noted that the film containing the fiber had relatively few cracks compared with the flakes formed after calcination by the deposition of the titanium precursor on a glass slide without the fibers [43].

3.2 Assemblies

Here the templating of an assembly of biological cells that have a fiber-like structure with an ordered inner arrangement and gels of organogelators, which also have a fibrous structure, are discussed. Both nanocasting and nanocoating can be achieved in the first example, whereas the use of organogel templates showed controlled nanocoating, giving inorganic hollow fibers upon heating.

3.2.1 *Biological Threads*

Cylindrical bacterial filaments, formed by the growth of cylindrical shaped cells of *Bacillus subtilis*, are drawn from solution to form this template. The structure is composed of the filaments aligned along the direction of the thread and packed in a hexagonal fashion. This bacterial superstructure has been infiltrated with preformed silica nanoparticles [44]. The negatively charged particles could infiltrate the swollen macroscopic threads as binding with the anionic cell walls is inhibited. (The charge on the nanoparticles plays an important role in the use of this template, since positively charged titania and alumina particles did not infiltrate the fiber but coated its outer surface with a uniform layer [44].) On drying the silica particles are retained with 50 and ~200 nm thick walls formed between the filaments and in the voids, respectively. Aggregation and condensation of hydroxyl groups on removal of the organic template gave a fiber structure with an inverse morphology to the template: ordered macroporous channels (0.5 μm diameter) were found to run parallel along the direction of the thread.

This cellular assembly has also proven a good template for the fabrication of hierarchical pore structures by penetrating the thread with an aqueous tetraethylorthosilicate (TEOS)/hexadecyltrimethylammonium bromide/base solution. The resulting material on removal of the filaments and added porogen gave ordered macropores with periodic mesoporous silica walls [44]. Here the final structure indicated a nanocoating of the individual filaments composing the thread compared to the previous example where a nanocasting of the structure was obtained.

3.2.2 *Organogelators*

Organogelators are low molecular weight organic compounds that can gel solvents at low concentrations. Terech and Weiss [45] have recently reviewed

organogelators and their properties. In general, the gel is formed by heating the gelator in an organic liquid and then cooling, which leads to fibrous aggregation of the organic compound. Hybrid fibers and, on removal of the organic materials, hollow inorganic fibers have been formed by the addition of inorganic precursor molecules to the organogel and solvent. The mechanism proposed is initially the formation of the gel, followed by electrostatic attraction of the metal oxide oligomers and continued polymerization of the metal oxide to form the coating; see Scheme 3. Hence the organic superstructures that are held together by noncovalent interactions can be permanently fixed in inorganic materials.

Ono et al. [46] showed that silica coated organic fibers could be obtained when TEOS was polymerized in the presence of a cholesterol-based gelator that contained quaternary ammonium groups. The absence of this functionality did not give the same results, as the cationic groups on the fibrils allowed the ad-

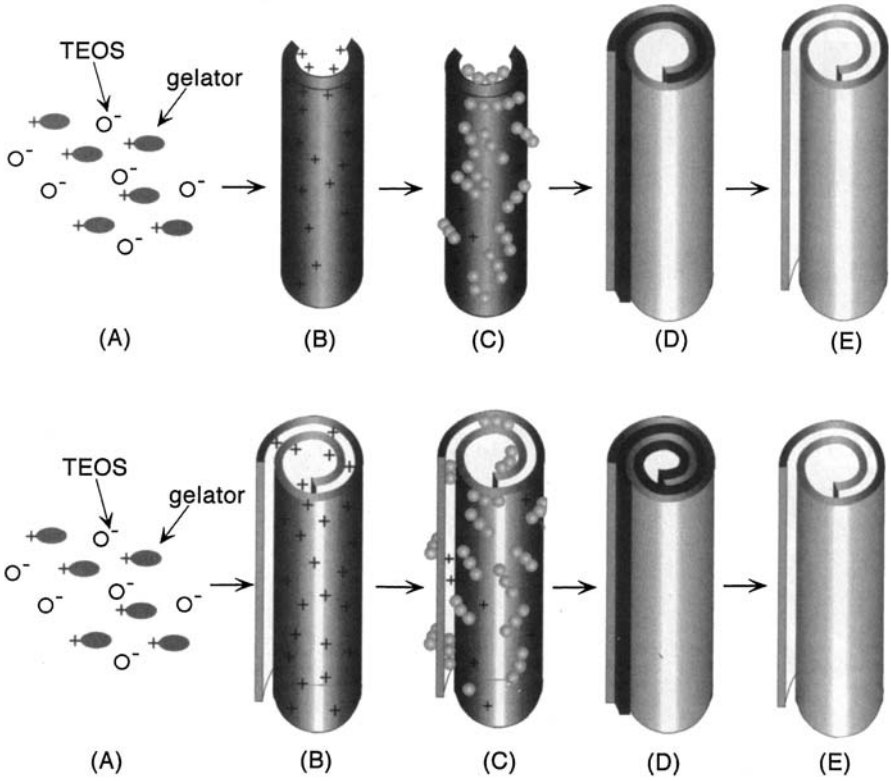

Scheme 3A–E. Mechanism of inorganic coating of organogelators. Schematic representation for the creation of paper-like roll silica by sol-gel polymerization of TEOS in the organogel state of 4: **A** mixture of gelator and TEOS; **B** gelation; **C** sol-gel polymerization of TEOS and adsorption onto the cationic gelator; **D** before calcination; **E** paper-like roll multilayer structure of the silica formed after calcination. Reprinted with permission from [49]. Copyright 2000 American Chemical Society

sorption of the anionic silica oligomers where polymerization could then continue along the fibril. Hollow silica fibers were formed on removal of the gelators by calcination. The addition of an azacrown moiety to the cholesterol based gelator required high salt concentrations to produce a hollow silica material as the final product, again due to electrostatic coupling between the template and condensing silica [47]. Variation of the final silica structure, i.e., wall thickness, surface texture, and a tubular or "rolled paper-like" structure could be obtained by changing the salt concentration and the type of crown ether added to the gelator, which effected the organogel superstructure [48, 49]. Hydrogen bonding interactions [50] between gelator superstructures and silica were also successful in the formation of hollow silica structures.

Titania hollow fibrous structures can be formed as well by the use of organogel templates through either electrostatic or hydrogen bonding interactions between the template and the titanium compound [51, 52]. Calcination at 450°C removes the organogel giving hollow anatase or anatase/rutile titania fibers with lengths of up to 200 μm and outer diameters between 150 and 1200 nm. The titania materials consist of crystalline nanoparticles (diameter 15–30 nm) compared with the silica structures, which remain amorphous.

Chirality can be induced into the silica structure by the use of either a cholesterol based gelator with an azacrown moiety in the presence of metal cations [53] or organogels comprised of chiral diaminocyclohexane derivatives [54]. Helical ribbons and double layered nanotubes (diameter ~500 nm) composed of titania can also be obtained [55].

The sol-gel transcription of organogels has been extended to sugar integrated gelators showing structural versatility [56], monodisperse inner diameters [57], and control of the inner diameter [58]. Single fibers, "lotus-type" fiber structures, or spherical superstructural aggregates can be formed. These structures can then be transcribed into silica by sol-gel polycondensation giving single or multiple hollow fiber structures or spherical structures [56]. Inorganic hollow fibers with rather monodisperse inner diameters of 5 or 9 nm (outer diameter ~50 nm) can also be obtained [57]. Control over the inner diameter of the final inorganic tube was dependent on gelator concentration, with inner diameters of 20–25 nm for 0.1 wt% and 450–600 nm for 3 wt% obtained [58].

Diazocrown appended cholesterol gelators formed vesicular aggregates that have also been templated [59]. The spherical silica structures obtained had two distinct diameters, ~200 nm (interconnected spheres) and ~2500 nm (isolated spheres) which closely resembled the initial gelator assembly. Poly(L-lysine), which also forms spherical aggregates (in the presence of a hydrophobic base additive), can be templated to give, as the end product, hollow silica spheres of various diameters [60]. As yet no attempts have been made to control the aggregate size.

The formation of hierarchical pore structures in the silica has also been achieved by the use of a gelator 2, 3-di-*n*-decyloxyanthracene in methanol [61]. Hollow fibers with micron-sized diameters are obtained on removal of the gelator, which contain mesopores from smaller gelator aggregates. Changes in the mesopore diameter (5–12 nm) and shape (ink-bottle or cylindrical) occur for different gelator concentrations.

4
Discrete Entities

Individual submicron entities can be cast to form monolithic structures with voids that maintain the initial organic shape (as was discussed above), or they can be coated to give individual hybrid entities that form hollow inorganic structures on removal of the template. The particles, tubes, and crystals are generally dispersed in solution for templating.

4.1
Spherical Particles

A number of inorganic materials have been coated on polymer spheres, which can be obtained with a variety of diameters and compositions. The inorganic coating results in significant changes of the sphere properties. The organic core can also be removed to form hollow inorganic spheres. Porous polymer spheres have also been templated to produce non-agglomerated, porous inorganic beads.

4.1.1
Solid Latex Particles

As polymer spheres are easily accessible with low polydispersity, they are attractive templates. Coating in non-aqueous solvents is usual as most metal alkoxide precursors rapidly undergo hydrolysis and condensation in the presence of water.

Silica coatings on PS spheres (2.3 μm) were obtained in ethanol [62]. The microspheres that were prepared in the presence of poly(vinyl pyrrolidone), PVP, were dispersed in ethanol, to which water, base, and TEOS were added. Seeded polymerization of TEOS on the surface of the spheres (as well as free silica particle formation in solution) led to a coating composed of silica nanoparticles (30–40 nm). After centrifugation and drying the coating step could be repeated. An increase in the silica coating from 7.8 to 18.5 wt% was obtained after one and three coatings, respectively. Hollow silica spheres could be obtained after burning off the PS at 600°C.

Shiho and Kawahashi [63] showed that amorphous titania can be coated on PS spheres. Titanium tetrabutoxide (TBOT) is hydrolyzed in the presence of anionic PS spheres (diameter 420 nm) and PVP as a protective agent by aging at 100°C. Centrifugation and redispersion cleaned the system to give coated spheres with a coating thickness of ~60 nm. If there was an excess of TBOT, separate TiO_2 particles formed in solution. When the dried samples were calcined at 600°C, hollow anatase titania spheres were obtained. Using higher temperatures during calcination (900°C) resulted in phase transformation to the rutile crystal and these crystal particles no longer maintained the hollow spherical structure.

Zhong et al. [64] have shown that the cell designed for fabricating colloidal crystals and their metal oxide inverse can also be used for the formation of

amorphous inorganic coated polymer spheres and hollow inorganic spheres. The crystalline PS array formed between the glass substrates is dried and then infiltrated with dilute precursor solution (for example, TIP:isopropanol, 1:19 v/v or tin-tetraisopropoxy:ethanol 1:19 v/v), which leads to separation of the spheres. On exposure to atmospheric moisture a homogeneous, dense, thin layer of amorphous material (TiO_2 or SnO_2) is coated on the PS beads. Immersing the hybrid material in toluene leads to dissolution of the PS giving hollow amorphous spheres that can be released from the substrate by sonication. The wall thickness was found to be dependent on the polymer sphere diameter and the concentration of the precursor. Hollow spheres were not formed when silica precursors were used due to the longer gelling time, which meant that solvent evaporation occurred before complete gelation, and hence a 3D porous structure was formed. Egg-shaped PS particles, which were prepared by deformation of monodisperse spheres embedded in an elastic matrix, were also coated with titania using a similar set-up [65]. Wall thickness (between 30 and 100 nm) was again dependent on the precursor concentration. Removing the PS by immersion in toluene gave ellipsoidal TiO_2 shells.

Titania can also be coated on cationic PS spheres (diameter 378 nm) in solution by a one-step process [66]. The PS spheres dispersed in ethanol with PVP are rapidly stirred during the addition of the titania precursor in ethanol. The slight negative charge on the titania species ensures their rapid capture by the positive PS spheres, preventing the formation of TiO_2 particles in solution. Thicker coatings can be obtained by varying the PS to titania precursor ratio or by carrying out repeated titanium isopropoxide additions. After centrifugation and redispersion to remove the PVP, smooth titania coatings on homogeneous spheres are obtained. Removing the core using either solvent extraction (toluene) or calcination leads to the formation of hollow TiO_2 spheres. In the case of heating the sample there is some damage to the shells, which consist of mainly anatase crystals.

Preformed metal oxide nanoparticles have been successfully coated on polymer spheres by the use of the layer-by-layer method. This involves the coating of the template spheres with polyelectrolyte layers, which are oppositely charged to the metal oxide nanoparticles to be deposited. Alternating the polyelectrolyte and nanoparticle deposition has led to the successful formation of silica [67, 68] and titania [69] coated PS spheres. Using this approach preformed crystalline nanoparticles can be deposited on the organic spheres and crystalline hollow spheres can be obtained without the need of calcination. On removal of the template and the polymer interlayers by heating, hollow spheres of the inorganic material can be obtained [68–70]. This procedure is described in detail in the chapter by Dr Frank Caruso.

4.1.2
Porous Spheres

Porous polymer spheres with a range of diameters, pore sizes, and composition (or surface functionality) can be purchased. Antonietti et al. have shown that porous polymer spheres could be cast to form monolithic materials [33]. Water-

swollen polystyrene sulfonate spheres were cast in an aqueous TMOS/HCl solution. The other latices that had been used in this procedure gave spherical pores on removal of the organic material as casting occurred around the particles (see Sect. 2.2.1); however, these polystyrene sulfonate spheres were infiltrated by the precursor solution and subsequent polyreaction, followed by removal of the organic spheres, gave a mesoporous silica material without spherical pores.

Instead of casting the complete solution to form a monolith, individual porous spheres can be templated to form porous inorganic beads, which maintain porosity from the template. As with any of the discrete organic templates, experimental conditions need to be optimized to ensure that aggregation of the beads does not occur and that there is not excess inorganic material forming on the template surface.

PS cross-linked with divinylbenzene beads, with diameters of either 15 or 30 μm that could also be functionalized with hydroxy or amine groups, were impregnated with precursor, for the fabrication of titania spheres, before being placed in excess water for hydrolysis and condensation reactions to occur [71]. To form silica porous spheres the silica precursor was added to an acidic aqueous solution containing the beads, and the system was heated at 70°C. On calcination the polymeric material was removed giving the inorganic spheres with inner pores. The surface functionality of the beads played an important role in the success of templating with the non-functionalized beads being most suitable for the titania, and the hydroxy or amine groups being required for silica sphere formation. Images of the titania spheres, obtained from SEM and TEM are shown in Fig. 6.

4.2 Elongated Materials

Biological tubes of high aspect ratio, including phospholipid tubes and tubular structures formed by the tobacco mosaic virus, and the inorganic materials obtained by templating them, are described first before moving to a smaller scale, the templating of carbon nanotubes. Organic crystals are also included in this section as they have been used successfully to give hollow elongated inorganic structures.

4.2.1 *Tubes and Nanotubes*

Chiral phospholipid molecules aggregate spontaneously to form tubes with diameters of 500 nm and lengths of ~50–100 μm. Diacetylenic phosphatidylcholine structures were first coated in 1993 by Baral and Schoen [72] with silica nanoparticles. The tubule dispersion was mixed with Ludox (a silica sol with a particle diameter of 10–15 nm and negative surface charge at pH 8.2) and allowed to stand for up to 9 days, during which time a white precipitate formed. TEM analysis of the collected precipitate showed a film with a thickness of about 50 nm, composed of silica particles, on the hollow cylindrical templates. The adsorption of the nanoparticles to the headgroups of the phospholipid is believed

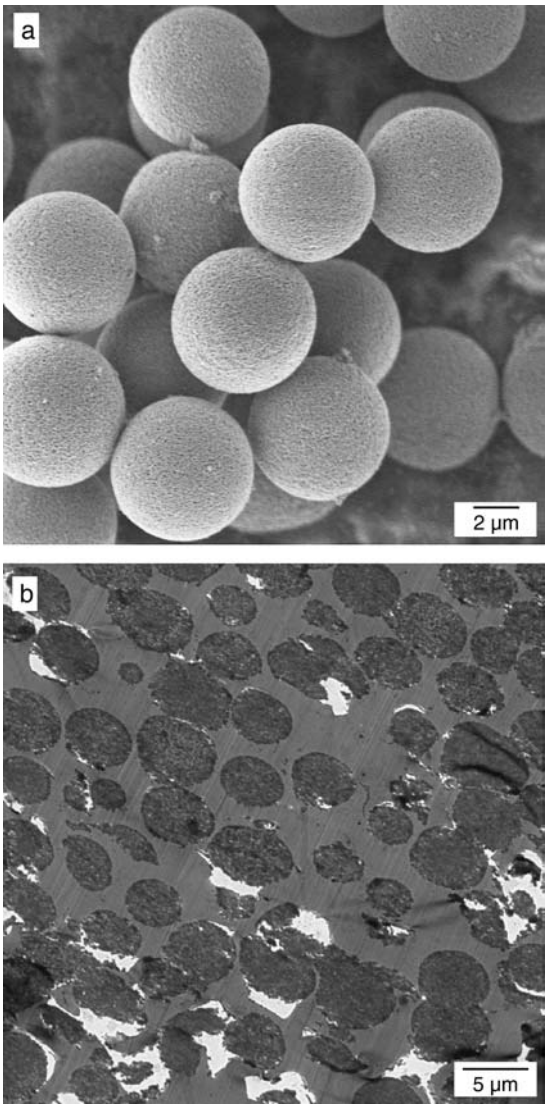

Fig. 6. **a** SEM image and **b** TEM image of the porous titania spheres obtained on templating of PS cross linked with divinyl benzene porous beads. Adapted with permission from [71]. Copyright 2002 Wiley-VCH

to be due to electrostatic interactions. Heating can be used to remove the tubules, giving hollow cylindrical silica materials with lower aspect ratios (length decreases to 15–25 μm). This structure is different to that obtained by simultaneous phospholipid crystallization and silica polymerization, where helical silica-lipid multilamellar microstructures were obtained [1].

The tobacco mosaic virus is a hollow protein nanotube with inner and outer diameters of 4 and 18 nm, respectively, and lengths of 300 nm [73]. The virus is stable over a range of pH values and has been used as a template for the formation of inorganic-organic hybrid nanotubes with reaction pHs ranging from 2.5 to 9. These tubular structures were templated using sol-gel chemistry. A silica coating of 3 nm formed on the outer surface of the tobacco mosaic virus tube when a suspension of the hollow tubes was mixed with an acidified TEOS/ethanol solution [73]. TEM analysis showed that the white precipitate obtained is composed of longer silica coated nanotubes due to end-to-end self assembly of the virus.

Carbon nanotubes with inner diameters of 2–8 nm and lengths of up to 1 μm have been used for the fabrication of both metal oxide nanotubes and nanorods, as well as having application in the coated form. Satishkumar et al. [74] used multiwalled carbon nanotube templates for the formation of silica, alumina, and vanadium oxide nanotubes. After stirring the carbon nanotubes in the precursor solutions (TEOS, aluminum isopropoxide/H_2O, or a vanadium pentoxide gel) the solids obtained were heated to give inorganic coatings on the organic nanotubes. Further heating under air leads to the removal of carbon, giving well preserved SiO_2 and V_2O_5 tubes. The tubular structure was not well maintained for Al_2O_3 on removal of the template.

Zirconia nanotubes were also obtained using a similar method with a zirconium propoxide precursor [75]. After oxidizing the carbon, zirconia tubes with a diameter of ~40 nm, 6 nm wall thickness, and several micrometers long were obtained. The ZrO_2 was composed of mixed crystal phases (monoclinic and tetragonal). Increased temperature treatment led to collapse of the nanotubes. The addition of yttria in a slightly modified procedure gave a more stable nanotube structure with similar wall thicknesses. The yttria-stabilized zirconia had a cubic structure.

Extending the work further to other oxides gave V_2O_5, WO_3, MoO_3, RuO_2, and IrO_2 coated carbon nanotubes [76]. TEM images of some examples are shown in Fig. 7. However, on removal of the carbon, nanorods of V_2O_5, WO_3, MoO_3 (and with further treatment MoO_2), Sb_2O_5, RuO_2, and IrO_2 were formed. Nanotubes of MoO_3 and RuO_2 were also obtained. The nanorods had a range of diameters (from 10 to 200 nm) and lengths up to a few micrometers.

Nanoparticles have also been used for coating carbon nanotubes. The multiwalled carbon nanotubes (average length 50 μm) were combined with a silica sol that was prepared by mixing the silane precursor (either methyl, ethyl, or propyl-trimethoxysilane) with ethanol and hydrochloric acid [77]. After thorough mixing and then drying, a porous film exhibiting fibrous structures is obtained. Varying the amount of sol added to the carbon nanotubes resulted in different loading amounts of silica to carbon. The electrochemical properties of the composite film also altered with changes in silica to carbon nanotube composi-

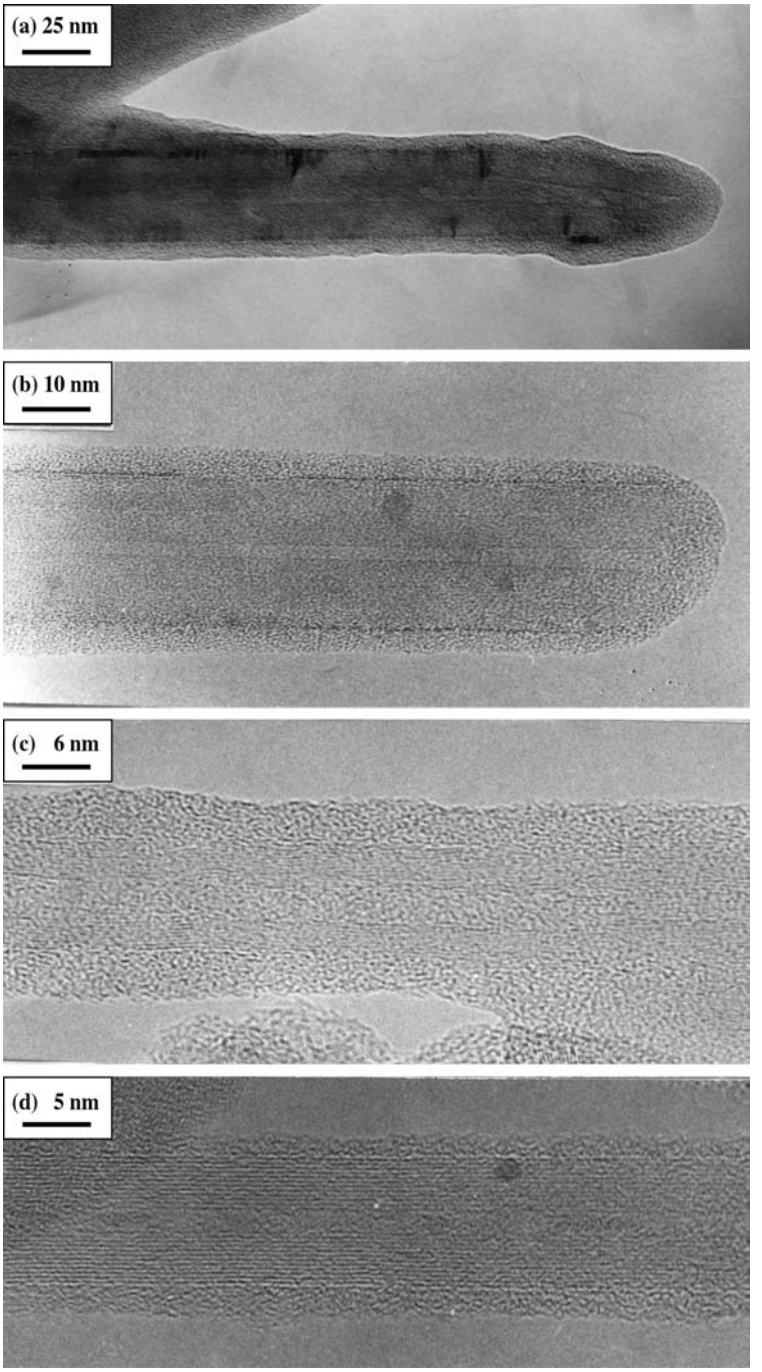

Fig. 7a–d. Metal oxide coated carbon nanotubes: **a** SiO_2; **b** V_2O_5; **c** WO_3; **d** MoO_3. Adapted with permission from [76]. Copyright 2000 The Royal Society of Chemistry

tion with reduction in double layer capacitance with either increasing silica concentration or increasing chain length of the alkoxide.

4.2.2 *Organic Crystals*

Ammonium *dl*-tartrate crystallizes in ethanol to give needle-like crystals, which can be used as templates for surface specific sol-gel polymerization [78]. The addition of NH_4OH to an ethanol solution containing TEOS and *dl*-tartaric acid gave a precipitate. As ammonium *dl*-tartrate crystals are soluble in water, the water formed on silica condensation and the water washing of the precipitate removes the template to yield smooth, open-ended silica tubes (length 200–300 μm) with wall thicknesses ranging from 30 to 300 nm [79, 80]. The size of the tubes could be varied by the addition of base to solution before the silica precursor. Triangular- or rectangular-shaped (0.7–6.5 μm wide), elongated silica structures (length 50–100 μm) could also be obtained by the crystallization of ammonium oxalate hydrate [78].

5 Summary

The examples given in this chapter demonstrate how organic materials of various structure can be utilized for the formation of either novel hybrid systems or structured metal oxide materials by nanocasting or nanocoating techniques. The two procedures discussed – (i) the use of sol-gel polymerization within or around the organic mold and (ii) nanoparticle infiltration and adhesion to the organic mold – have been used to form structured porous monoliths, films, and individual entities composed of metal oxide or hybrid materials. Composite structures can have significantly different properties to both the organic and inorganic starting materials. On removal of the organic template, novel inorganic structures are produced with structural properties that can lead to enhanced performance or new applications. For example, lower densities, larger surface areas, ordered pore systems, film or monolith formation, and higher flow throughput are beneficial in numerous applications. In general, porous metal oxide materials with controlled structure formation can be used in catalytic applications, chromatography, as containers for encapsulation and delivery, fillers, in quantum optics, as sensors, separators, in solar energy applications, or as pigments for paper or paints.

Fabrication of new organic templates with interesting structures coupled with further control of the ordering or dispersity of current templates will be a prime task for future application of nanocasting and nanocoating techniques.

Acknowledgement. CNR Rao is thanked for providing original photos for Fig. 7. Jan H. Schattka is especially appreciated for assistance with figure preparation. Markus Antonietti, Frank Caruso, Atul Deshpande, Michael Giersig, Andreas Greiner, Hans-Peter Hentze, Anders Larsson, Ulrika Meyer, Helmuth Möhwald, Jan H. Schattka, Dmitry G. Shchukin, and Andrei Susha are thanked for fruitful discussions and collaborations. The Max Planck Society is acknowledged for funding.

References

1. Mann S, Burkett SL, Davis SA, Fowler CE, Mendelson NH, Sims SD, Walsh D, Whilton NT (1997) Chem Mater 9:2300
2. Brinker CJ, Scherer GW (1990) Sol-gel science: the physics and chemistry of sol-gel processing. Academic Press, California
3. Yoldas BE (1986) J Mater Sci 21:1086
4. Rouquérol J, Avnir D, Fairbridge CW, Everett DH, Haynes JH, Pericone N, Ramsay JDF, Sing KSW, Unger KK (1994) Pure Appl Chem 66:1739
5. Antonietti M, Göltner C, Hentze H-P (1998) Langmuir 14:2670
6. Antonietti M, Caruso RA, Göltner CG, Weissenberger MC (1999) Macromolecules 32:1383
7. Caruso RA, Giersig M, Willig F, Antonietti M (1998) Langmuir 14:6333
8. Caruso RA, Antonietti M, Giersig M, Hentze H-P, Jia J (2000) Chem Mater 13:1114
9. Schattka JH, Shchukin DG, Antonietti M, Caruso RA (2002) Chem Mater 14:5103
10. Breulmann M, Davis SA, Mann S, Hentze H-P, Antonietti M (2000) Adv Mater 12:502
11. Caruso RA, Schattka JH (2000) Adv Mater 12:1921
12. Caruso RA, Antonietti M (2002) Adv Funct Mater 12:307
13. Stein A (2001) Microporous Mesoporous Mater 44/45:227
14. Blanford CF, Yan H, Schroden RC, Al-Daous M, Stein A (2001) Adv Mater 13:401
15. Velev OD, Jede TA, Lobo RF, Lenhoff AM (1997) Nature 389:447
16. Velev OD, Jede TA, Lobo RF, Lenhoff AM (1998) Chem Mater 10:3597
17. Holland BT, Blanford CF, Stein A (1998) Science 281:538
18. Wijnjoven JEGJ, Vos WL (1998) Science 281:802
19. Yang P, Deng T, Zhao D, Feng P, Pine D, Chmelka BF, Whitesides GM, Stucky GD (1998) Science 282:2244
20. Park SH, Qin D, Xia Y (1998) Adv Mater 10:1028
21. Holland BT, Blanford CF, Do T, Stein A (1999) Chem Mater 11:795
22. Gundiah G, Rao CNR (2000) Solid State Phys 2:877
23. Yi G-R, Moon JH, Yang S-M (2001) Chem Mater 13:2613
24. Subramania G, Constant K, Biswas R, Sigalas MM, Ho K-M (1999) Appl Phys Lett 74:3933
25. Subramania G, Manoharan VN, Thorne JD, Pine DJ (1999) Adv Mater 11:1261
26. Subramania G, Constant K, Biswas R, Sigalas MM, Ho K-M (1999) J Lightwave Technol 17:1970
27. Meng Q-B, Gu Z-Z, Sato O, Fujishima A (2000) Appl Phys Lett 77:4313
28. Meng Q-B, Fu C-H, Einaga Y, Gu Z-Z, Fujishima A, Sato O (2002) Chem Mater 14:83
29. Gates B, Yin Y, Xia Y (1999) Chem Mater 11:2827
30. Park SH, Xia Y (1998) Chem Mater 10:1745
31. Park SH, Xia Y (1998) Adv Mater 10:1045
32. Akin FA, Zreiqat H, Jordan S, Wijesundara MBJ, Hanley L (2001) J Biomed Mater Res 57:588
33. Antonietti M, Berton B, Göltner C, Hentze H-P (1998) Adv Mater 10:154
34. Jiang P, Bertone JF, Colvin VL (2001) Science 291:453
35. Martin CR (1996) Chem Mater 8:1739
36. Lakshmi BB, Patrissi CJ, Martin CR (1997) Chem Mater 9:2544
37. Patrissi CJ, Martin CR (1999) J Electrochem Soc 146:3176
38. Patrissi CJ, Martin CR (2001) J Electrochem Soc 148:A1247
39. Chia S, Urano J, Tamanoi F, Dunn B, Zink JI (2000) J Am Chem Soc 122:6488
40. Bognitzki M, Hou H, Ishaque M, Frese T, Hellwig M, Schwarte C, Schaper A, Wendorff JH, Greiner A (2000) Adv Mater 12:637
41. Bognitzki M, Czado W, Frese T, Schaper A, Hellwig M, Steinhart M, Greiner A, Wendorff JH (2001) Adv Mater 13:70
42. Caruso RA, Schattka JH, Greiner A (2001) Adv Mater 13:1577
43. Caruso RA, Greiner A (unpublished results)
44. Davis SA, Burkett SL, Mendelson NH, Mann S (1997) Nature 385:420
45. Terech P, Weiss RG (1997) Chem Rev 97:3133

46. Ono Y, Nakashima K, Sano M, Kanekiyo Y, Inoue K, Hojo J, Shinkai S (1998) Chem Commun 1477
47. Ono Y, Kanekiyo Y, Inoue K, Hojo J, Shinkai S (1999) Chem Lett 23
48. Jung JH, Ono Y, Shinkai S (1999) J Chem Soc Perkin Trans 2:1289
49. Jung JH, Ono Y, Shinkai S (2000) Langmuir 16:1643
50. Jung JH, Ono Y, Shinkai S (2000) Chem Lett 636
51. Kobayashi S, Hanabusa K, Hamasaki N, Kimura M, Shirai H, Shinkai S (2000) Chem Mater 12:1523
52. Kobayashi S, Hanabusa K, Suzuki M, Kimura M, Shirai H (1999) Chem Lett 1077
53. Jung JH, Ono Y, Shinkai S (2000) Angew Chem Int Ed 39:1862
54. Jung JH, Ono Y, Hanabusa K, Shinkai S (2000) J Am Chem Soc 122:5008
55. Jung JH, Kobayashi H, von Bommel KJC, Shinkai S, Shimizu T (2002) Chem Mater 14:1445
56. Jung JH, Amaike M, Nakashima K, Shinkai S (2001) J Chem Soc Perkin Tran 2 10:1938
57. Tamaru S-I, Takeuchi M, Sano M, Shinkai S (2002) Angew Chem Int Ed 41:853
58. Jung JH, Shinkai S, Shimizu T (2002) Nano Lett 2:17
59. Jung JH, Ono Y, Sakurai K, Sano M, Shinkai S (2000) J Am Chem Soc 122:8648
60. von Bommel KJC, Jung JH, Shinkai S (2001) Adv Mater 13:1472
61. Clavier GM, Pozzo JL, Bouas-Laurent H, Liere C, Roux C, Sanchez C (2000) J Mater Chem 10:1725
62. Bamnolker H, Nitzan B, Gura S, Margel S (1997) J Mater Sci Lett 16:1412
63. Shiho H, Kawahashi N (2000) Colloid Polym Sci 278:270
64. Zhong Z, Yin Y, Gates B, Xia Y (2000) Adv Mater 12:206
65. Lu Y, Yin Y, Xia Y (2001) Adv Mater 13:271
66. Imhof A (2001) Chem Mater 13:3579
67. Caruso F, Lichtenfelder H, Giersig M, Möhwald H (1998) J Am Chem Soc 33:8523
68. Caruso F, Caruso RA, Möhwald H (1998) Science 282:1111
69. Caruso RA, Susha A, Caruso F (2001) Chem Mater 13:400
70. Caruso F, Caruso RA, Möhwald H (1999) Chem Mater 11:3309
71. Meyer U, Larsson A, Hentze H-P, Caruso RA (2002) Adv Mater 14:1768
72. Baral S, Schoen P (1993) Chem Mater 5:145
73. Shenton W, Douglas T, Young M, Stubbs G, Mann S (1999) Adv Mater 11:253
74. Satishkumar BC, Govindaraj A, Vogl EM, Basumallick L, Rao CNR (1997) J Mater Res 12:604
75. Rao CNR, Satishkumar BC, Govindaraj A (1997) Chem Commun 1581
76. Satishkumar BC, Govindaraj A, Nath M, Rao CNR (2000) J Mater Chem 10:2115
77. Gavalas VG, Andrews R, Bhattacharyya D, Bachas LG (2001) Nano Lett 1:719
78. Miyaji F, Davis SA, Charmant JPH, Mann S (1999) Chem Mater 11:3021
79. Nakamura H, Matsui Y (1995) J Am Chem Soc117:2651
80. Nakamura H, Matsui Y (1995) Adv Mater 7:871